Design of Functionally Graded Materials via Metal Additive Manufacturing

Team Members: Naat'anii Castillo, Nhung Nguyen, Faith Rolark

Summary

Traditional graded materials are composed of multiple phases that are noted by sharp changes in microstructure, thermophysical and material properties which can generate high stresses along the material interface boundary that may initiate delamination, cracks, and other defects. To solve this problem, the composite material can be designed to have a gradual variation in their composition, microstructure, or properties. These functionally graded materials (FGM) are controlled smooth variations that endows the material with specific properties that vary throughout its dimensions. FGMs have prominent applications in aerospace, defense, automotive and biomedical industries, where there is an increased demand to manufacture optimized, high-performance parts. The advent of additive manufacturing allows for increased flexibility for prototyping low-volume customized parts with shorter processing times. Directed energy deposition (DED) is one of the most common metal additive manufacturing technologies that utilizes a high-power laser to melt deposited powder on a substrate. The DED process is highly customizable, as the quantity of deposited powder can be modified to allow for multi-material parts, which would enable the on-demand fabrication of FGMs. Here, we propose to design a FGM consisting of Inconel 718 and Niobium. Niobium, a rare earth metal, is often used to improve the mechanical properties of Nickel based alloys such as the Inconel alloy family. Adding the Niobium element to Inconel would precipitate the γ"-phase to enhance the tensile strength and creep at high temperatures. However, Niobium also can be segregated at the grain boundary to form the Laves phase at elevated temperature, then depletes the alloy strength. Therefore, an investigation on the microstructure evolution of Inconel-Niobium alloy is essential to the evaluation of its mechanical properties.

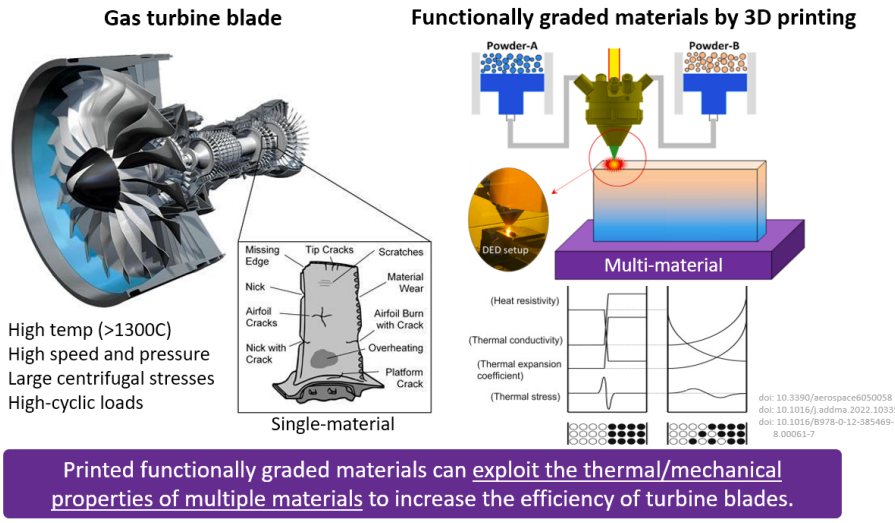

Figure 1: Proposed application of functionally graded materials for high-temperature turbine blades.

System Design Chart

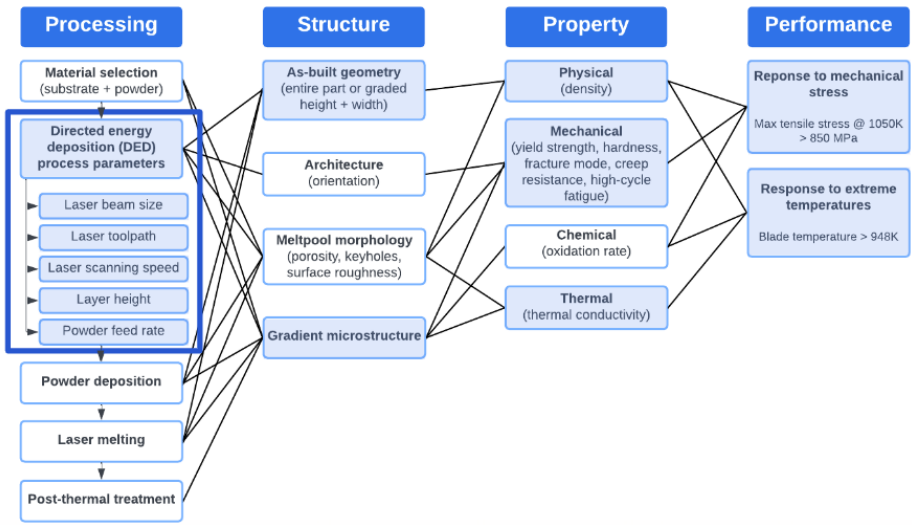

Figure 2: System design for fabricating functionally graded materials via the directed energy deposition process with a focus on process design.

The system design chart as Figure 2 shows the relationship between processing, structure, properties, and performance. As the critical requirement for jet engine components, the as-printed part must work at extreme temperatures and respond to stress. Therefore, mechanical properties such as high strength, creep resistance, and fatigue resistance at high frequency are vital. The high-temperature working condition also accelerates the oxidation process. Hence, the chemical property, e.g., oxidation rate, should be considered. In addition, the physical and thermal property also included in the design process with the favoring of lightweight material with high thermal conductivity.

Processing and microstructure are critical factors in achieving the above mention properties and performance. Additive manufacturing is a popular process to build complex geometries for jet engine components. Here, the directed energy deposition (DED) is chosen to fabricate the element with the control of laser beam size, scan speed, tool path, layer height, and powder feed rate. By adjusting these factors, many structural aspects can be attained, such as geometry, architecture, morphology, and gradient microstructure. Amongst them, the gradient microstructure, including the gradient increment of element composition ratios, is the main focus of this study. The gradient increment of the Niobium element in Inconel 718 with the gradient change in microstructure is expected to respond to the different mechanical stress of the component in working conditions.

Materials Selection

AM Processing on Microstructure

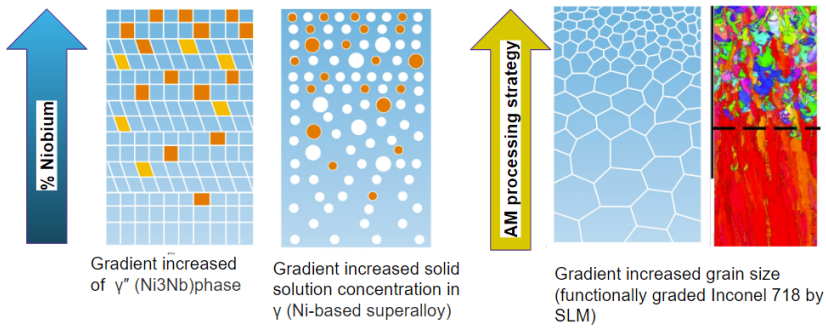

Figure 3: Effects of graded Niobium on phase precipitation in Ni-based superalloy [1]. Grain refinement of functionally graded IN718 as a result of selected laser melting process [2].

The addition of Niobium content into the Inconel 718 by Additive Manufacturing can create gradient structure based on the chemical and structure gradient. Increment Niobium content using a layer-by-layer approach generate the gradient of Niobium concentration in solid solution of the FCC γ phase. Adding excess amount of Niobium amount will promote the precipitation of the strengthening γ'' or the brittle Laves phases, then fabricate the gradient in volume of these phases. In addition, the change in concentration of element also leads to the changes in grain sizes by differ the kinetic reactions. Moreover, the adjustment in Additive Manufacturing process also can help to tailoring the texture and grain size. Popovich *et al.* proposed the functionally graded Inconel 718 processed by additive manufacturing with different regions of fine and coarse grained microstructure [2]. This work suggests the feasibility of processing strategy for functional performance relating to the change in microstructure.

Service Temperature

The maximum service temperature indicates the most extreme functional temperature that designed turbine blades are capable of withstanding. This study focuses on first-stage turbine blades, which are

placed directly after the combustion chamber. As such, the turbine blades are exposed to the highest temperature by the ignited fuel-air mixture pushed from the combustion chamber. During the startup of gas turbine operations, the turbine inlet commonly reaches a maximum temperature of 1350°C [3]. Figure 4 provides an illustration of the maximum service temperature for fan blades, compressor blades, and turbine blades for specific tensile strengths. This study focuses on materials that are suitable for turbine blades under these high-temperature environments. This selection of materials includes Stainless Steel 316L, Hastelloy X, and Inconel 718, among others [4].

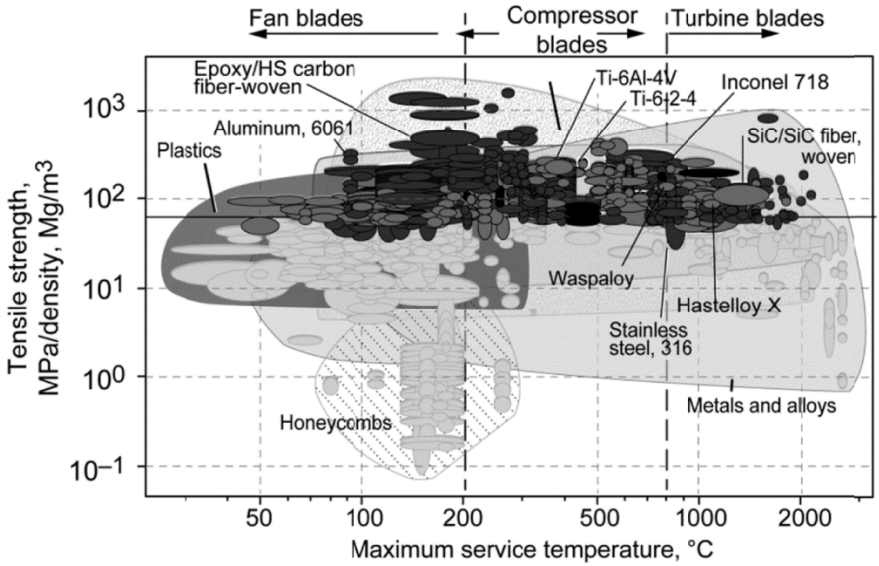

Figure 4: Maximum service temperatures of specific tensile strengths for materials suited for fan, compressor, and turbine blades [4].

Specific Tensile Strength

Turbine blades experience sustained stresses as a result of their operation; therefore, it is important to consider the limits of a material's ability to withstand tensile stress before fracture occurs. This property is a key mechanical strength metric as a material with a high tensile strength is better able perform under high cyclical loading and high centrifugal forces. This translates to a longer operational lifetime for the turbine blades and reduces the need for frequent maintenance or replacement.

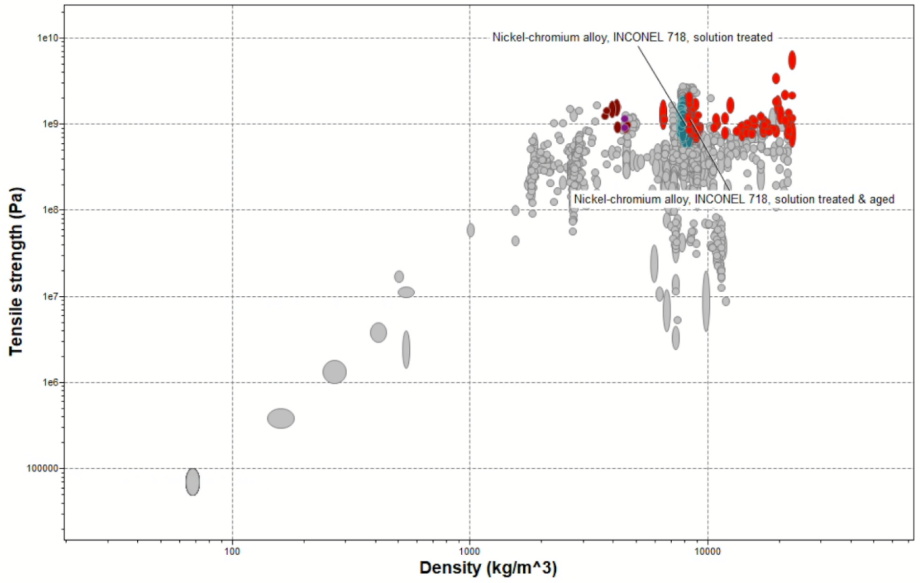

Figure 5: Tensile strength and density for materials with a greater tensile strength of 850 MPa, maximum service temperature of 1350 C, and excellent oxidation resistance at 500 C.

Specific Fracture Toughness

Turbine blades are subjected to high centrifugal forces and high cyclical loading that may make the material susceptible to crack propagation and cause failure. In order to assess the stability of a material in these conditions, the fracture toughness of prospective materials will be considered. The fracture toughness characterizes a material's resistance to the propagation of crack, or other deformations, under applied stress.

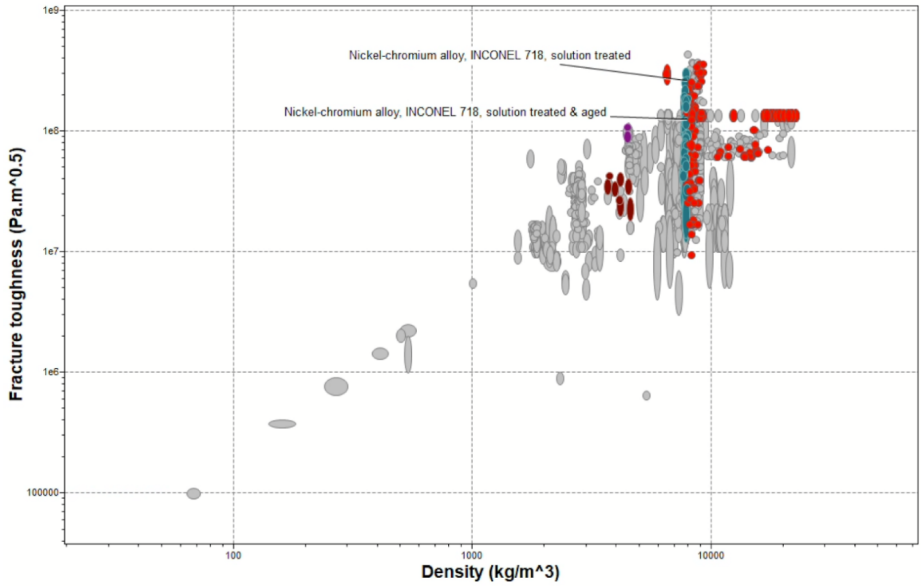

Figure 6: Fracture toughness and density for materials with a greater tensile strength of 850 MPa, maximum service temperature of 1350 C, and excellent oxidation resistance at 500 C.

Oxidation Resistance

The turbine blade works at high-temperature typically above 1000 C. At this operation temperature, the surface oxidation is accelerated and becomes the critical factor in reducing the time service of the blade. Oxidation resistance can be improved by some alloying elements such as Cr and Al to form the protective oxide layer. The Cr2O3 can improve the oxidation resistance at moderate temperatures (up to 900 C). Adding Al with approximately 6wt% into the alloy at higher operating temperatures can form the protective oxidation Al2O3 [reference]. Therefore, the Inconel 718, with a high fraction of Cr and Al components, will be a good material for the turbine blade [5]. Experimental work showed that Inconel 718 oxidation rates at 900 C and below atmospheric pressure are minimal, with no measurable weight gain from oxidation after 24 hours. At a higher temperature regime from 950 C to 1300 C, Inconel 718 displayed parabolic oxidation rate dependence for up to several weeks [6].

Price

The cost is always remaining the crucial factor for considering the materials in design for production. The Ashby chart shows the ratio of cost versus the yield strength from various of super alloys and Ni-based alloys. It shows that IN718 have the good combination of low price (about $120 per kg) and the high yield strength of 1000 MPa.

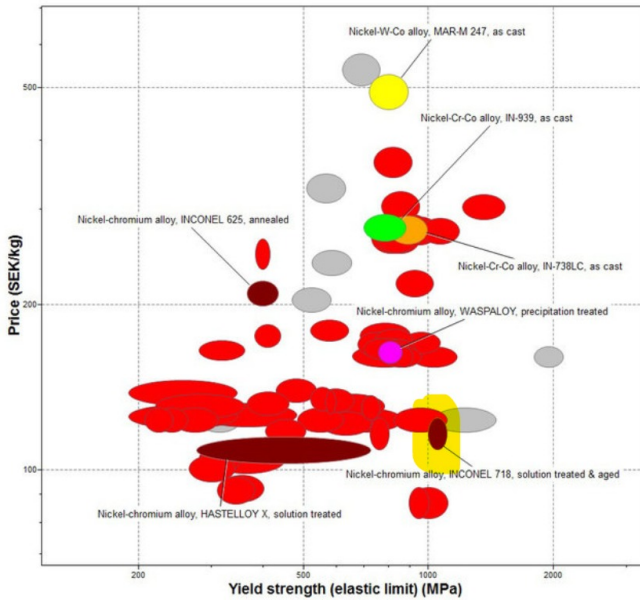

Figure 7: Ashby diagram comparing cost and yield strength of common superalloys [7].

Property	Requirement
Tensile Strength	≥850 MPa
Maximum Service Temperature	1350 ℃
Corrosion Resistance	Excellent
Oxidation Resistance	Excellent

Design Approach

Experimental Workflow

The workflow of the experimental process is outlined in Figure 8. The experimental process consists of four steps of material preparation, printing, sample preparation, and characterization.

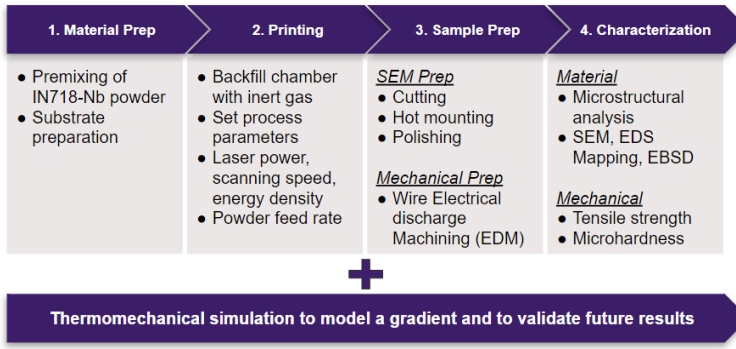

Figure 8: Experimental workflow for the preparation, fabrication, and characterization of a 3D-printed build.

Material Preparation

A blend of IN718-Nb powder was premixed and loaded into a single hopper. The composition was a ratio of 100:4.4g IN718 to Nb (resulting in a final content of 9wt.% Nb). Premixing was done separately and prior to the mixing that occurs within the powder delivery system since the built-in mixer can only adjust material output in steps of 0.1 RPM (~10g/min), which would yield compositions with excessive Niobium (>10 wt.% Nb) . By premixing the Niobium powder with IN718, lower percentages of Niobium can be achieved in the final material gradient.

Experimental Printing Setup

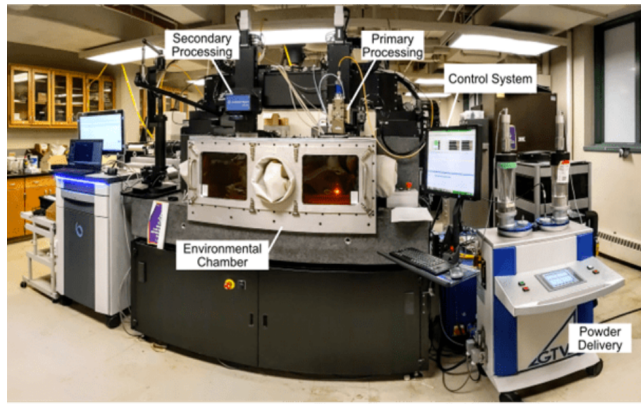

Figure 9: Experimental setup of the Additive Rapid Protoyping Instrument (ARPI) for the fabrication of printed structures.

A custom additive manufacturing setup (Additive Rapid Prototyping Insturment, ARPI) was used to facilitate experimental printing. The setup was used to perform directed energy deposition (DED), a 3D printing technique where powder is deposited onto a substrate and is immediately melted and fused together via a high-powered laser to form 3-dimensional structures. The laser employs a continous wave at a wavelength of λ = 450 nm with a laser processing unit (Precitec). This laser processing unit is composed of a coaxial nozzle, where a laser beam is directed through the center of the nozzle and powder is deposited through the coaxial ring. The motion of the laser processing head is controlled by a cartesian motorized stage (Aerotech). Powder was stored in two separate hoppers and fed into a powder delivery system (Fraunhofer) that can mix powders together at varying mass flow rates.

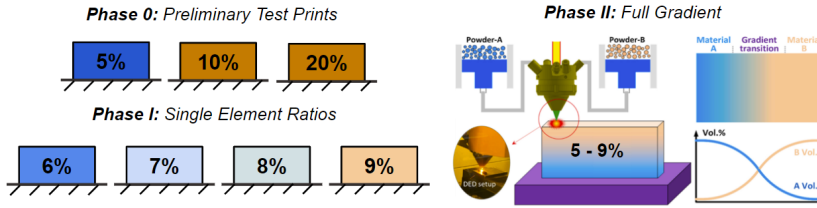

Figure 10: Experimental phases of the project. Phase 0 consists of preliminary test prints, phase I includes printing thin-walls composed of a single element composition ratio, and Phase II involves printing a full gradient thin-wall [8].

The laser parameters were set based on the laser settings to form a stable melt pool for a pure IN718 build. This was done because the majority of the resulting powder mixture will be primarily composed of IN718 relative to the Nb content in the mixture. The laser was set to 500 W with a scanning speed of 7 mm/s and a layer height of 0.33 mm to build a 30 mm thin-wall of 30 total layers. The laser parameters are outlined in Table 1.

Table 1: Baseline laser parameters for IN718 thin-wall builds.

Power	Spot dia.	Standoff	Scan Spd.	Wall Len.	Layer Ht.	Layers
500 W	1.4 mm	10 mm	7 mm	30 mm	0.33 mm	30 layers

For the following experiments, the loaded powder in the custom setup consisted of pure IN718 in Hopper A and an IN718-Nb mixture in Hopper B (See Material Preparation Section). The elemental composition ratios and accompanying mass flow mixing settings are shown in Table 2.

Table 2: Powder mass flow rate settings for thin-wall build experiments.

Exp No.	wt.% Nb	IN718-Nb Flow Rate [g/min]	IN718 Flow Rate [g/min]
1	5%	0	10
2	10%	1	10
3	20%	2	1
4	6%	2	8
5	7%	4	6
6	8%	6	4
7	9%	8	2
8	5-9%	0 to 1	1 to 0

Sample Preparation

The samples will be prepared for two main purposes: characterization and mechanical testing. In order to analyze the microstructure of the alloys, the samples will be mounted with a conductive material in a hot mounter and subsequently polished for a mirror finish. The sample preparation for samples that will undergo mechanical testing will involve sectioning with a wet saw to create samples of equal dimensions.

Microstructural Characterization

A scanning electron microscope (SEM) will be used to characterize the spatial distribution of phases within the alloy samples. An image may be captured using the backscatter electron (BSE) detector to highlight the areas with Niobium content. The energy dispersive x-ray spectroscopy (EDS) feature of the SEM will be used to understand the concentration of elements throughout the sample. This method will be a more rigorous approach to understanding the elemental distribution and may help with phase identification.

Mechanical Characterization

In order to evaluate the performance of the fabricated alloys, the characterization of their mechanical strength is necessary to understand how the addition of Niobium impacts the performance of the material within

the context of turbine blade application. Tensile strength was selected as a metric of interest since turbine blades undergo this type of loading during their operation. As turbine blades spin, they experience cycles of tension and compression during each rotation. Obtaining a value for the maximum tensile load tolerated by the samples may give insight into the operational lifetime of the alloy if it were in use. The second metric used to characterize the samples is microhardness. Hardness measurements are useful when evaluating the mechanical stability of a material as it measures the material's resistance to plastic deformation. Microhardness is especially insightful for evaluating the design of alloys because it can provide information regarding the material's microstructure by mapping hardness values across different regions of the sample which may contain different phases. This testing may give information about the mechanical behavior of the different phases that result from the addition of Niobium to Inconel 718.

Results and Discussion

Microstructural Analysis

Inconel 718 (IN718) is the Face-Centered Cubic (FCC) niobium-modified precipitation-hardened nickel-iron alloy with the nominal composition of Ni (50-55%), Cr (17-21%), Mo (2.8-3%), Ti (0.65-1.15%), Co (1%), Nb (4.8-5.5%) and Fe (balance). The microstructure of IN718 contains the FCC matrix (γ phases), strengthening carbides (MX (Nb,Ti)(C, N)), and intermetallics such as FCC γ' Ni_3(Al,Ti,Nb) and ordered tetragonal γ" Ni_3Nb phases. The microstructure of IN718 also concludes some undesired phases such as hexagonal laves $(Ni, Fe, Cr)_2$(Nb,Mo,Ti), orthorhombic δ Ni_3(Nb,Ti), and tetragonal σ CrFe phases. Of these undesirable phases, the laves phase is particularly concerning because this brittle intermetallic compound can strongly degenerate the mechanical properties of IN718 (ref)**??**. However, some specific thermal treatments are often used to dissolve the unfavorable laves phase and increase the phase ratio of strengthen phases γ' and γ". Inconel 718 (IN718) is the Face-Centered Cubic (FCC) niobium-modified precipitation-hardened nickel-iron alloy with the nominal composition of Ni (50-55%), Cr (17-21%), Mo (2.8-3%), Ti (0.65-1.15%), Co (1%), Nb (4.8-5.5%) and Fe (balance). The microstructure of IN718 contains the FCC matrix (γ phases), strengthening carbides (MX (Nb,Ti)(C, N)), and intermetallics such as

FCC γ' Ni_3(Al,Ti,Nb) and ordered tetragonal γ" Ni_3Nb phases. The microstructure of IN718 also concludes some undesired phases such as hexagonal laves $(Ni, Fe, Cr)_2$(Nb,Mo,Ti), orthorhombic δ Ni_3(Nb,Ti), and tetragonal σ CrFe phases. Of these undesirable phases, the laves phase is particularly concerning because this brittle intermetallic compound can strongly degenerate the mechanical properties of IN718 [9]. However, some specific thermal treatments are often used to dissolve the unfavorable laves phase and increase the phase ratio of strengthen phases γ' and γ".

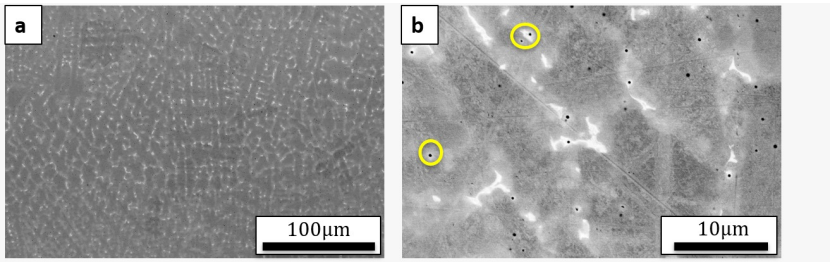

Figure 11: The BSE image of microstructure in IN718. (a) The microstructure of IN718 with γ matrix (grey) and laves phase (white), (b) Yellow circles mark some representative pores. The laves phases are homogeneously distributed in the matrix. The size of laves phase is estimated from 1 to 10 μm.

The BSE microstructural images of IN718 by DED are presented in Figure 11. It shows the γ matrix (grey) and laves phase (white). The alloy has many pores (in yellow circles), as shown in Figure 11b. The laves phase is homogeneously distributed in the matrix with irregular shapes and sizes in the range of 1-10 μm (Figure 11c). The volume fraction of laves phase is estimated at 5%. Laves phase volume fraction is reported as 3.5-15% in IN718 by laser DED with a high cooling rate [10, 11]. The volume fraction of laves phase in IN718 by DED manufacturing is notably higher than in the casting method, with laves phase volume is approximately 1.2-2% [12]. It leads to an apparent relation between laves phase volume and solidification rate. Therefore, adjusting processing parameters, particularly the solidification rate, in AM production is a factor in the produce gradient microstructure with the function of laves phase volume fraction.

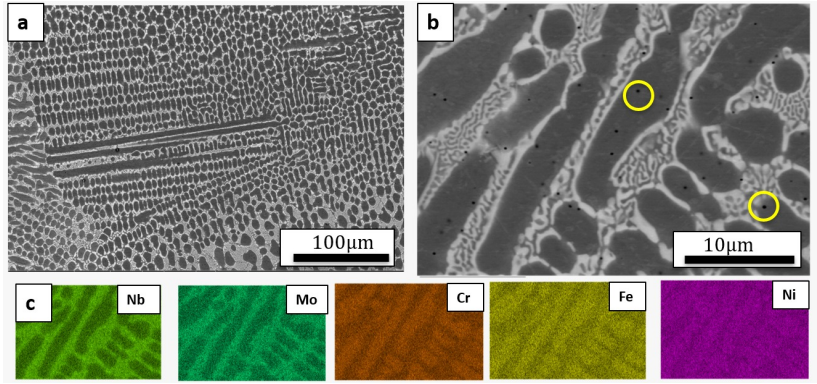

Figure 12: The BSE and EDS elemental mapping image of microstructure in IN718-10Nb. (a) The Dendrite morphology of laves phase is in the network-like structure. (b) The Yellow circles mark some representative pores. The EDS elemental mapping confirms the network-like structure of laves phases, with laves phase enriched in Nb and Mo elements.

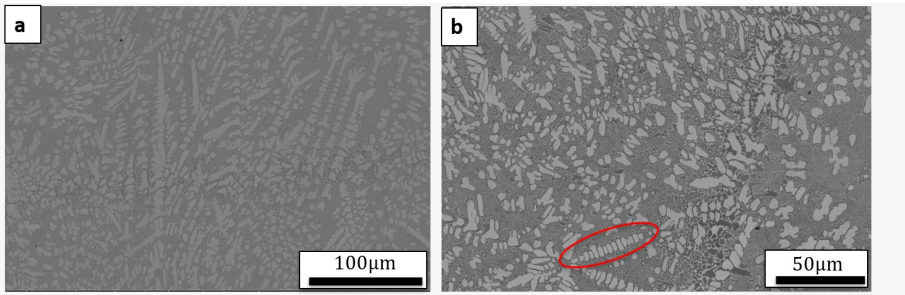

Figure 13: The BSE microstructural image of IN178-20Nb. (a) The Dendrite morphology of laves phase (b) The dendrite structure with the chain-like structure (in red circle) at some position.

The BSE microstructural and EDS elemental mapping images of Nb-addition to IN718 are displayed in Figures 12 and 13. Both samples show dendrite morphology with a characteristic of columnar grain. However, there was a marked difference in the microstructure of IN718 with 10% Nb (IN718-10Nb) and IN718 with 20% Nb (IN718-20Nb). In the IN718-10Nb sample (Figure 12), the dendrite morphology of laves phase is in the network-like structure (Figure 12b) with the confirmation of EDS elemental mapping in Figure 12c, as in consensus to the research of IN718 with 11% Nb addition by laser DED [13]. In contrast, the IN718-20Nb microstructure (Figure 13) displayed the dendrite structure with

the chain-like structure at some positions, as shown in Figure 13b [13]. The size of laves phase in IN718-20Nb is also notably larger than those in IN718-10Nb, resulting from an increment in Nb content. In addition, the volume fraction of the laves phase is also highest in the IN718-20Nb sample. Heat treatment in IN718-10 Nb and IN718-20 Nb can dissolve the laves phases. The Nb concentration from the partial dissolution of the Laves phases is again back to γ matrix to form the strengthening γ" phase in the interdendritic region [9]. Moreover, the Nb element also had a lower diffusion rate to not create Nb micro-segregation at the high cooling condition of DED. As a result, the increased concentration of Nb element in γ matrix forms the solid solution to strengthen the alloy. Another point is the lattice distortion caused by the mismatch between atomic size difference and the short-range internal stress between γ matrix and Nb solute atoms. Therefore, adding Nb in IN718 can promote the hardness and tensile properties through various strengthening mechanisms [9, 13] However, the fracture toughness of Nb augmented IN718 is decreased by the interface instability between the laves phase and the austenite γ matrix and from the brittle laves phases. The research on the corrosion behavior of Nb augmented IN718 by laser melting deposit was carried out with electrochemical tests, including electrochemical impedance spectroscopy and potentiodynamic polarization [14]. Adding Nb in IN718 also supports corrosion resistance, particularly improvement in pitting corrosion. This positive finding is attributed to the carbide precipitates due to the strong affinity between niobium and carbon.

Temperature-Displacement Model

A coupled temperature-displacement model was simulated to determine the potential thermomechanical effects a printed part may experience under extreme operating conditions. ABAQUS was used to generate the graded model. The part was partitioned into 5 distinct sections, where it was graded for 5, 6, 7, 8, 9 wt.% Nb (from bottom-up). The material property values used are shown in Figure 14, which displays a diagram of the simulated model.

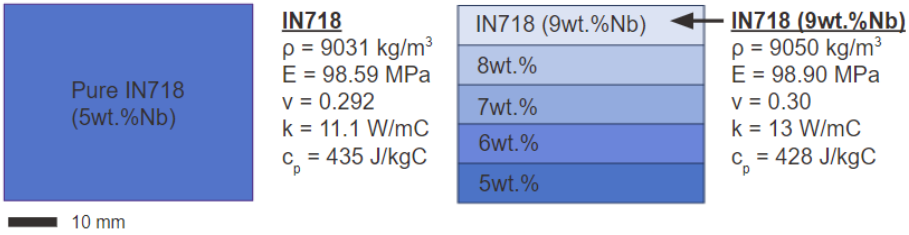

Figure 14: Diagram of the simulated graded part with material properties for 5 and 9wt.% Nb.

The boundary conditions for the model included a fixed bottom edge and temperature at 1000 C at the same location. The loading conditions considered the most extreme case for the functional turbine environment. A maximum operating stress of 1000 MPa and a calculated heat flux of 14000 W/m (based on a service temperature of 1350 C) was applied to the top edge. These values were previously defined in the materials selection portion of this study.

Figure 15 shows the simulated temperature gradient of a potential printed part. It is noted that there are sharp changes in gradient for each of these partitions as this models an as-built printed sample. The gradient is constant throughout each partition and large incremental changes in temperature are made as heat dissipates downward. Under steady-state conditions, the temperature linearly decreases from 1350 to 1000 C. This behavior is displayed in Figure 16. Further studies can compare discretized parts with finer gradients.

The von Mises stress distribution of the simulated wall is shown in Figure 17. The stress gradually descends as the load travels further down the part. Drops in stress were observed for height positions 18 and 24mm, as this is the interface between two different partitions. The stress distribution is curvilinear because the center of the part undergoes slightly larger amounts of deformation, which results in a greater surface area and is inversely proportional to mechanical stress. The simulated part was able to endure at least 850 MPa of load, which is the required tensile strength of this part.

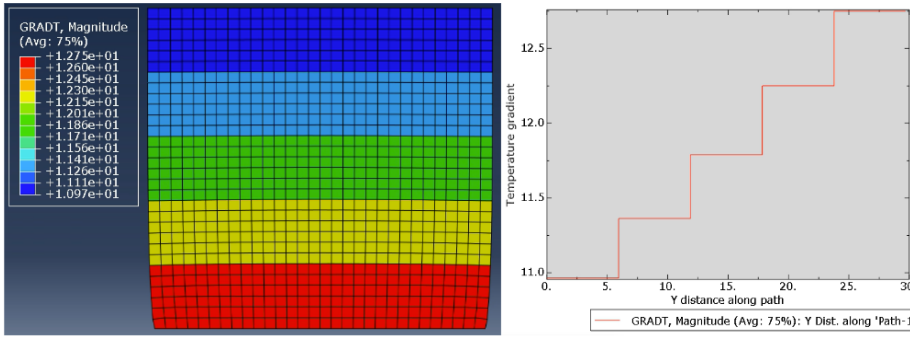

Figure 15: Temperature gradient of a wall consisting of five distinct grades.

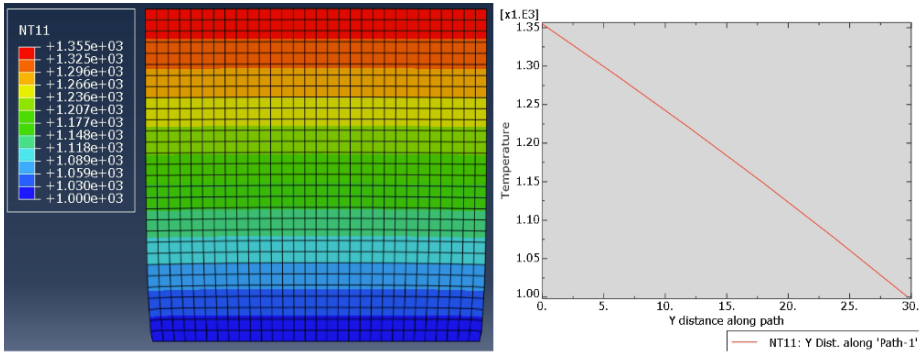

Figure 16: Modeled temperature distribution of a wall operating under turbine service conditions (up to 1350 C).

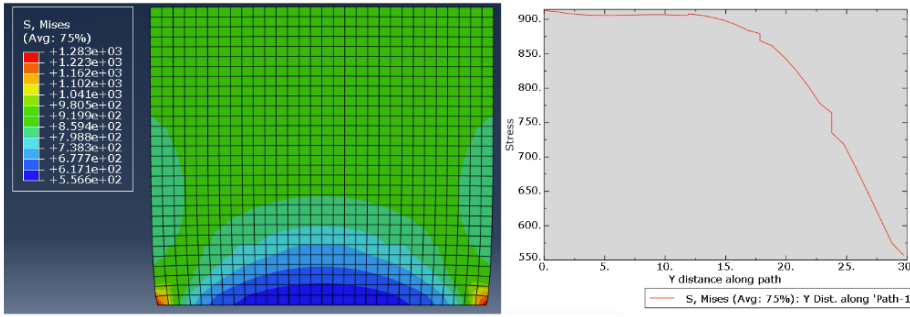

Figure 17: Stress distribution of wall enduring maximum expected turbine loads (1000 MPa).

Validation

As a validation of this work, it is recommended that both experimental and computational work should be done to verify the thermomechanical responses of the printed parts. Since it is difficult to print a true gradient from layer-by-layer 3D printing approaches, a fine gradient can be simulated to determine if the behavior of the printed graded parts are similar to that of real gradients. Additionally, further validation of this study can be done by printing materials with greater dissimilarity (such as printing composite materials). This would demonstrate the full capabilities of DED printing processes for manufacturing functionally graded parts.

Future Steps

Evaluating the microstructure of the preliminary samples is important to pinpoint defects or other undesirable features and develop hypotheses about how the processing may have resulted in these aspects. The next step would be to make adjustments to the parameters used to fabricate the samples. The goal of designing this functionally graded material is to create small enough step sizes between sections of different compositions such that these interfaces do not act as stress concentrators. This research also aims to assess the viability of using additive manufacturing as a primary technique to fabricate functionally graded materials since this method offers advantages to current methods. The main advantage of additive manufacturing is the high degree of control that users have over the design of their sample's microstructure. Characterization of the microstructure would also serve to build an understanding of how phases precipitate as the Niobium content changes with spatial orientation. It would be of interest to characterize these interfacial areas with SEM using backscattered electron (BSE) imaging and EBSD for phase identification. The BSE imaging would give information about the distribution of different phases and EBSD would provide information about volume fraction and crystallographic orientation that would aid in identifying these phases.

In order to assess the performance of the functionally graded alloy in comparison to pure Inconel 718, the samples may be subjected to tensile testing to find the maximum allowable loads and to identify the failure

sites. Imaging of the failure sites would allow for analysis of the failure mechanisms which may depend on how phases precipitate throughout the sample.

Contributions

Give a brief description of the contributions of each member of the team, as a list of bullet points

- Naat'anii: Sample preparation, materials selection, and property metrics
- Nhung: SEM microstructural characterization (BSE and EDS)
- Faith: Fabrication, simulation
- All: Report writing and deliverables

References

[1] X. Li, L. Lu, J. Li, X. Zhang, H. Gao, Mechanical properties and deformation mechanisms of gradient nanostructured metals and alloys, Nature Reviews Materials 5 (9) (2020) 706–723.

[2] V. A. Popovich, E. V. Borisov, A. A. Popovich, V. S. Sufiiarov, D. V. Masaylo, L. Alzina, Functionally graded inconel 718 processed by additive manufacturing: Crystallographic texture, anisotropy of microstructure and mechanical properties, Materials Design 114 (2017) 441–449.

[3] R. Z. Aminov, A. B. Moskalenko, A. I. Kozhevnikov, Optimal gas turbine inlet temperature for cyclic operation, Journal of Physics: Conference Series 1111 (1) (2018) 012046.

[4] S. M. Arnold, D. Cebon, M. Ashby, Materials selection for aerospace system, Tech. Rep. NASA/TM-2012-217411, National Aeronautics and Space Administration (2012).

[5] F. Palmert, Oxidation and degradation of nickel-base alloys at high temperatures, Master's thesis, KTH Industrial Engineering and Management, Stockholm, Sweden (2009).

[6] G. A. Greene, C. C. Finfrock, Oxidation of inconel 718 in air at high temperatures, Oxidation of Metals 55 (5) (2001) 505–521.

[7] A. S. Shaikh, Development of a ′ precipitation hardening ni-base superalloy for additive manufacturing, Master's thesis, Chalmers University of Technology, Gothenburg, Sweden (2018).

[8] W. Li, M. N. Kishore, R. Zhang, N. Bian, H. Lu, Y. Li, D. Qian, X. Zhang, Comprehensive studies of ss316l/in718 functionally gradient material fabricated with directed energy deposition: Multi-physics multi-materials modelling and experimental validation, Additive Manufacturing 61 (2023) 103358.

[9] L. Xu, Z. Chai, H. Chen, X. Zhang, J. Xie, X. Chen, Tailoring laves phase and mechanical properties of directed energy deposited inconel 718 thin-wall via a gradient laser power method, Materials Science and Engineering: A 824 (2021) 141822.

[10] S. Sui, J. Chen, Z. Li, H. Li, X. Zhao, H. Tan, Investigation of dissolution behavior of laves phase in inconel 718 fabricated by laser directed energy deposition, Additive Manufacturing 32 (2020) 101055.

[11] H. Xiao, S. Li, W. Xiao, Y. Li, L. Cha, J. Mazumder, L. Song, Effects of laser modes on nb segregation and laves phase formation during laser additive manufacturing of nickel-based superalloy, Materials Letters 188 (2017) 260–262.

[12] L. Ling, Y. Han, W. Zhou, H. Gao, D. Shu, J. Wang, M. Kang, B. Sun, Study of microsegregation and laves phase in inconel718 superalloy regarding cooling rate during solidification, Metallurgical and Materials Transactions A 46 (2015) 354–361.

[13] H. Liu, K. Guo, J. Sun, H. Shi, Effect of nb addition on the microstructure and mechanical properties of inconel 718 fabricated by laser directed energy deposition, Materials Characterization 183 (2022) 111601.

[14] X. Ni, L. Zhang, W. Wu, D. Zhu, D. Kong, C. Dong, G. Zhu, Functionally nb graded inconel 718 alloys fabricated by laser melting deposition: mechanical properties and corrosion behavior, Anti-Corrosion Methods and Materials 67 (1) (2020) 16–23.